Progress In Electromagnetics Research C, Vol. 85, 167–175, 2018

A Circularly Polarized Implantable Monopole Antenna for Biomedical Applications

Pujayita Saha*, Debasis Mitra, and Susanta K. Parui

Abstract—In this paper, a compact, circularly polarized printed monopole antenna is proposed at ISM band (2.4–2.48 GHz) for biotelemetry and implantable applications. The proposed antenna possesses a small dimension ($10 \times 10 \times 0.3\,\text{mm}^3$) and simple microstrip feeding structure. The circular polarization is easily achieved by introducing an "L" shape stub at the ground plane in ISM. The simulated 10 dB impedance bandwidth is around 13.87%, and 3 dB AR bandwidth is around 5.3%. The effect of different body phantoms is discussed to evaluate the sensitivity of the proposed antenna. The simulated peak gain of the proposed antenna is about -7.79 dBi across the operating band. The SAR analysis of the antenna configuration has also been studied.

1. INTRODUCTION

Due to the growing concern for human health and the convenience of medical care, implantable medical devices (IMDs) become a popular subject of research in recent years. The implantable devices are capable of providing continuous monitoring of various physiological parameters reducing the invasiveness of surgery. To communicate wirelessly between IMDs and external facilities, an implantable antenna is commonly required. However, designing an implantable antenna operating within the human body is very challenging as it must satisfy several constraints such as compact size, power consumption, lossy environment, polarization issues, wide operating bandwidth, sufficient radiation efficiency and foremost, the patient safety [1, 2].

Various types of implantable antennas such as planer inverted-F antenna (PIFA) [3, 4], helical antennas [5], loop antennas [6], slot antennas [7] have also been proposed. In [8, 9], multilayer configurations are used to reduce the antenna size. However, all the proposed antennas in the above-mentioned works either have larger footprints or are linearly polarized.

Due to different indoor multi-path effects and body postures, the RF telemetry of implantable devices greatly suffers from the polarization mismatch. Circularly polarized (CP) antennas, being insensitive to the antenna orientation constraints, are much more preferable as they reduce the polarization mismatch loss. Also, a single fed CP antenna is much more preferred due to its compactness than multi-feed antennas. However, designing a CP implantable antenna is a very challenging job as good circular polarization must be realized with limited size overcoming its inherent constraint of limited bandwidth [10]. Several works have been reported to achieve a single fed CP implantable antenna with sufficient AR bandwidth [11, 12, 13–15]. In most of the cases coaxial feeding structure has been used for implantable CP antennas. In [11], circular polarization was realized by the capacitive loading on the radiator operating at 2.4 GHz under the implantable condition. A CP loop antenna [12] is proposed at 902–928 MHz ISM band for implantable applications. By changing the position of feed and shorts, either right-hand circular polarization property or left-hand circular polarization property can be realized in

Received 18 May 2018, Accepted 3 July 2018, Scheduled 16 July 2018

* Corresponding author: Pujayita Saha (pujayita.2010@gmail.com).

The authors are with the Department of Electronics and Telecommunication Engineering, Indian institute of Engineering Science and Technology, Shibpur, India.

that design. AR (Axial Ratio) bandwidth of 18.2% was achieved for RHCP and LHCP configurations using shorting pins, truncated center square slot and slits, and the broadband impedance and AR features have been achieved in the implantable patch antenna [13] operating at the 2.4 GHz ISM band. The radiating element of the antenna in [14] consists of an annular ring and a central circular patch. The circular polarization is generated by adding a pair of open stubs in the inner boundary of the annular ring. In [15], the antenna structure is based on two identical orthogonal strips, each connected with one conformal L-strip. A shorting pin is introduced, bringing in a fundamental resonance at 1.4 GHz ISM band with linear polarization. Besides, with the adoption of the shorting pin, two extra resonant modes are excited and split in the higher band, generating two orthogonal electric fields with equal amplitude and $\pi/2$ phase difference, therefore, covering another ISM band at 2.45 GHz with circular polarization property. In all these reported works, the patch antenna with proper loading has been used as a CP radiator.

Printed monopole antenna becomes a major field of interest nowadays since it has its own advantages such as small size, omnidirectional radiation patterns, wide bandwidth and high radiation efficiency. Related works have been reported in [16–18] where the proposed antenna has been simulated and characterized in the free space environment. In [16], the proposed broadband monopole CP antenna consists of a C-shaped monopole with an open-loop placed on the backside. The rectangular vertical stub connecting to the ground plane is used to achieve wide impedance bandwidth and enhanced AR bandwidth of the antenna. The study of gain enhancement is done using a U-shaped ground plane to enhance the capacitive coupling and directivity and also to reduce the size of the antenna. In a CPW-fed CP monopole antenna [17], the CP is initially achieved by utilizing the asymmetric ground, and then a rectangular open loop is introduced to obtain wide-impedance bandwidth and broadband circular polarization characteristics. In [18], a CPW-fed dual-band and dual-sense monopole CP antenna has two rectangular parasitic elements and an I-shape grounded stub to achieve the desired circular polarization characteristics.

It is obviously clear that the proposed CP implantable antennas are majorly coaxially fed and large in volume in case of implantable situations. On the other hand, several monopole antennas were also proposed with considerable AR bandwidth, though being simulated in the free space environment. Hence, designing a CP implantable monopole antenna is still a subject of huge interest and challenge. In this paper, a miniaturized printed spiral monopole antenna has been proposed with an aim of using it in implantable medical devices. The novel features of this proposed antenna are its compact size with simple microstrip feeding structure, enhanced AR bandwidth, and high peak gain. The antenna design has been simulated in HFSS considering single layer, two layer and three layer tissue phantoms and then experimentally verified in skin mimicking gel.

2. ANTENNA DESIGN

As proposed in [16], a broadband C-shaped circularly polarized monopole antenna exhibits larger 10 dB impedance bandwidth and AR bandwidth which are achieved by properly placing a rectangular open loop coupled structure and a stub at the ground plane. However, its overall dimension makes it unsuitable for the medical applications, especially in implantable medical devices. Hence, the design of a compact implantable monopole antenna with acceptable impedance and AR bandwidth remains a challenge for the researchers. This paper presents a depiction of an ISM band implantable monopole antenna with circular polarization and simple microstrip line feed structures and impedance transformers. The design procedure and simulated results are discussed in the following section.

The design parameters of the proposed monopole antenna and its different dimensions are illustrated in Figure 1(a). The antenna is nested in an RT Duroid substrate (thickness = 0.3 mm, $\varepsilon_r = 10.2$, and loss tangent = 0.0035), and the reflection coefficient is simulated in a human skin environment to study the radiation characteristics at 2.45 GHz.

The overall dimension of the antenna is $10 \times 10 \times 0.3\,\text{mm}^3$. Microstrip feed line is used for feeding purpose. The width of the monopole is 0.4 mm. An 'L' shape stub is placed at the ground. The widths of the 'L' stub and L2 transformer are 0.5 mm and 0.56 mm, respectively. Photographs of the fabricated prototype are shown in Figure 1(b). The antenna parameters are given in Table 1.

The proposed antenna is embedded in three different body phantoms to evaluate its sensitivity as

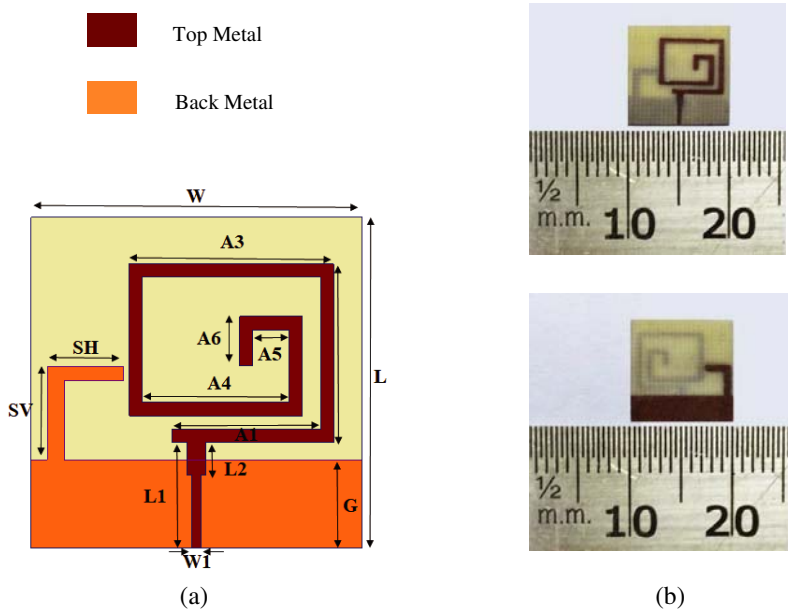

Figure 1. Geometry and photograph of the proposed implantable antenna. (a) Geometry of the designed antenna. (b) Fabricated antenna prototype (Top view and back view).

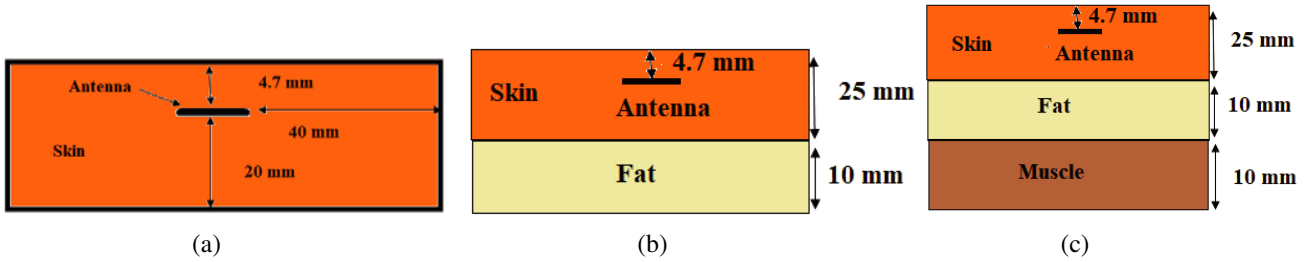

Figure 2. Simulation models: (a) One-layer tissue phantom. (b) Two-layer tissue phantom. (c) Three layer tissue phantom.

Table 1. Dimension of the proposed antenna (Unit: mm).

W	L	W1	L1	L2	A1	A2	A3	A4	A5	A6	G	SH	SV
10	10	0.28	3.2	1	4.5	5.3	6.1	4.54	1.1	1.5	2.65	2.3	3

shown in Figure 2. A simple single layer skin model with a dimension of 90 mm × 90 mm × 25 mm is considered to imitate the human tissue environment during simulation as shown in Figure 2(a). The other two phantoms considered here are two-layer body phantom (90 mm × 90 mm × 35 mm, Figure 2(b)) and three-layer body phantom (90 mm × 90 mm × 45 mm, Figure 2(c)). The antenna is then implanted in the skin at a depth of 4.7 mm in all the three cases and its upper surface directed towards the skin surface. The distance from the side of the structure to the edge of the skin is 4 cm at both sides. The dielectric properties of the tissues are frequency dependent and have the following values at 2.4 GHz. For skin it is $\varepsilon_r = 42.92$, $\sigma = 1.562$ S/m, for fat $\varepsilon_r = 5.285$, $\sigma = 0.012$ S/m, and for muscle $\varepsilon_r = 52.79$, $\sigma = 1.705$ S/m [19].

Two prototypes are used to explain the antenna design as shown in Figure 3. Antenna1 is a simple spiral printed monopole antenna with different arm lengths to achieve the desired resonant frequency in ISM band (Figure 3(a)). It is then further modified to Antenna2 to obtain the CP operation in the

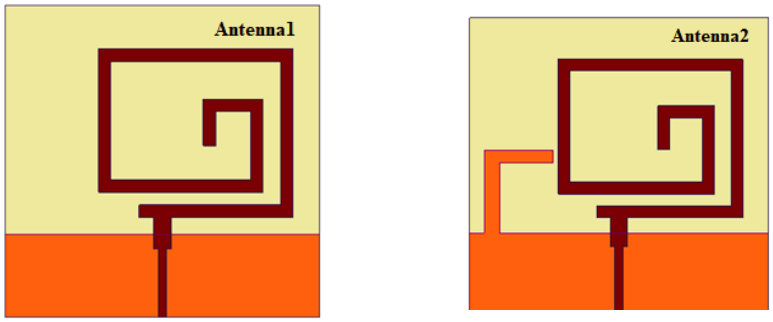

Figure 3. Prototypes of the proposed antenna. (a) Antenna without stub. (b) Antenna with stub.

said band (Figure 3(b)).

It is a well-known fact that, to realize the circular polarization, two orthogonal current components of equal magnitudes are required. The orthogonal arms of the monopole ensure a 90-degree phase difference between the two current components. The obtained CP is then fine-tuned by introducing an 'L' shaped stub in ground plane (Figure 3(b)). Surface current distributions on Antenna2 at 2.45 GHz at 0°, 90°, 180° and 270° phases as observed from $+z$ direction are depicted in Figure 4. It is observed that the current distributions at 180° and 270° are equal in magnitude and opposite in phase of 0° and 90°. It clearly shows that the current rotates in clockwise direction, and hence, LHCP is obtained at 2.45 GHz.

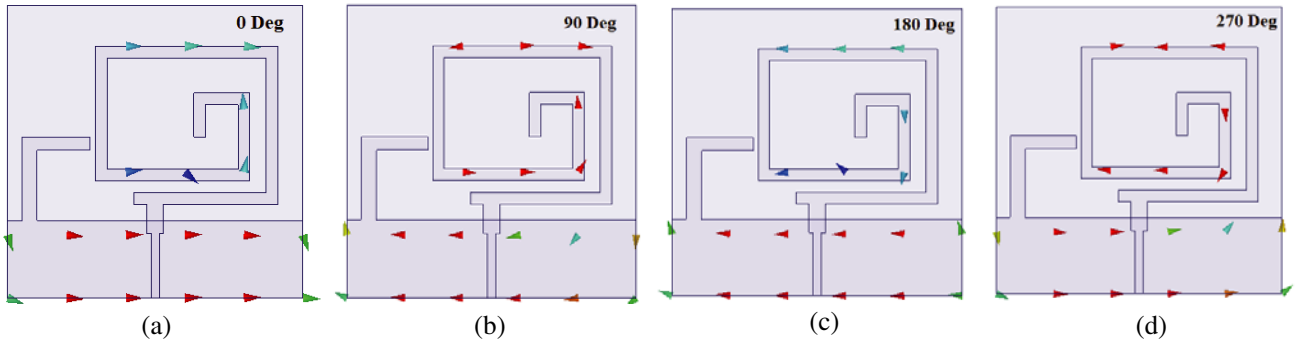

Figure 4. Surface current distribution at 2.45 GHz. (a) 0°. (b) 90°. (c) 180°. (d) 270°.

3. RESULTS AND DISCUSSION

3.1. Paramric Study

To identify the main factors affecting the performance of the proposed antenna and to achieve design guidelines, various key parameters are analyzed. Length of the monopole, being responsible for frequency shifting, is hence optimized to obtain the desired resonance frequency. Secondly, the height of the ground is coarsely tuned to efficiently optimize the structure. Both S_{11} and AR are more sensitive to the changes of "SH", the horizontal length of the stub (Figure 1(a)). Figure 5 represents the variation of S_{11} and AR with respect to SH. When SH = 2 mm, neither the impedance matching nor the CP mode has been observed in the ISM band. As soon as the antenna performance characteristics get close enough to the design specifications, the values of "SH' are finely adjusted, leading to an optimized 3-dB AR bandwidth from 2.42 to 2.48 GHz while allowing for a sufficient bandwidth with S_{11} lower than −10 dB.

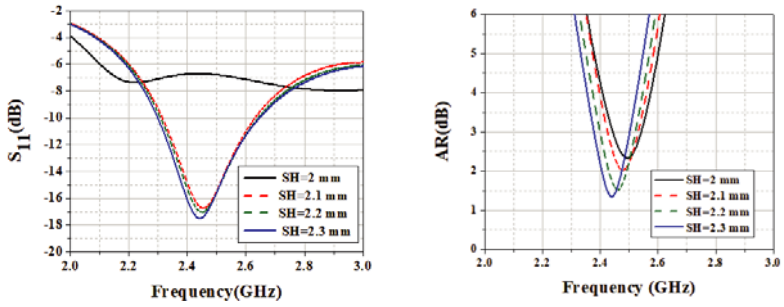

Figure 5. Effect of SH (horizontal length of the stub) on antenna performance: (a) S_{11}. (b) AR.

3.2. Reflection Coefficient

Figure 6 depicts the different simulation results of our proposed antenna. The simulated reflection coefficient (S_{11}) of the two prototypes in different phantoms is shown in Figure 6(a). Antenna1 resonates at 2.51 GHz whereas its modified version, Antenna2 (our proposed antenna) has 2.45 GHz as its resonant frequency. The simulated S_{11} and AR value of the proposed antenna in skin phantom are shown in Figure 6(b). Both the simulated -10 dB impedance bandwidth (2.30–2.64 GHz, 13.78%) and AR bandwidth (2.38–2.51 GHz, 5.30%) cover the entire ISM band. To estimate the sensitivity of the proposed antenna, it is then simulated in two different phantoms, and the corresponding results are shown in Figures 6(c) and 6(d). It is obviously clear from Figures 6(c) and 6(d) that both the S_{11} and AR value of the proposed antenna suffer minimum shift due to the change in the phantom model.

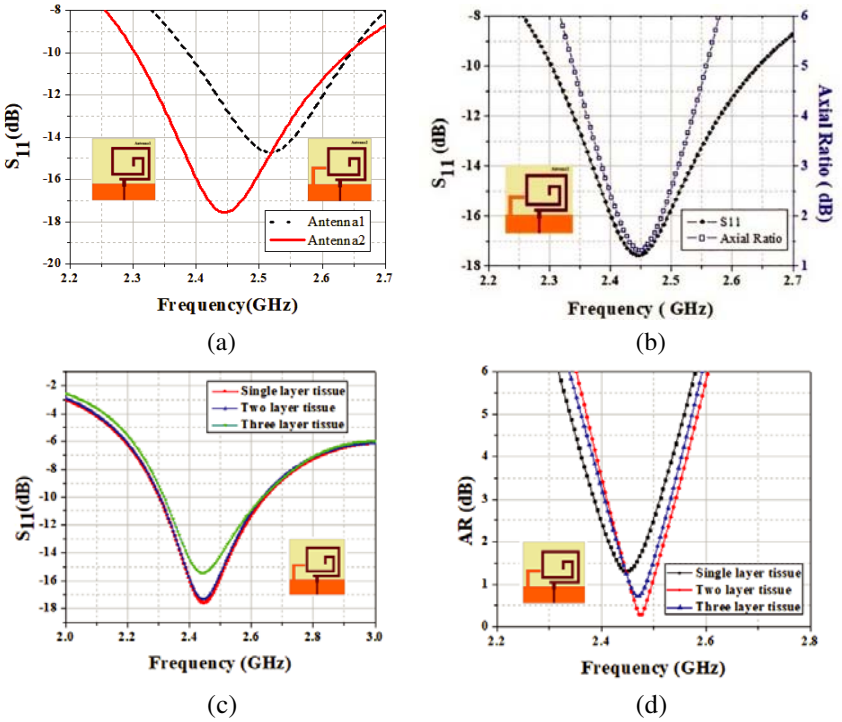

Figure 6. Simulated antenna charectaristics. (a) S_{11} of the Antenna1 and Antenna2 in skin phantom. (b) S_{11} and AR of Antenna2 in skin phantom. (c) S_{11} of Antenna2 for different phantoms. (d) AR of Antenna2 for different phantoms.

3.3. Gain

Figure 7 depicts the simulated gain of the proposed antenna. It is observed that the proposed antenna is of left-handed circular polarization (LHCP). The maximum LHCP radiation is toward the antenna's bore-sight at theta = 0°, which is the direction outward a human body. The right-handed circular polarization (RHCP) radiation is about 22 dBic lower than the LHCP one at theta = 0°. The realized gain in the single-layer skin phantom is −11.6 dBic. The simulated antenna efficiency is around 0.635% in ISM band.

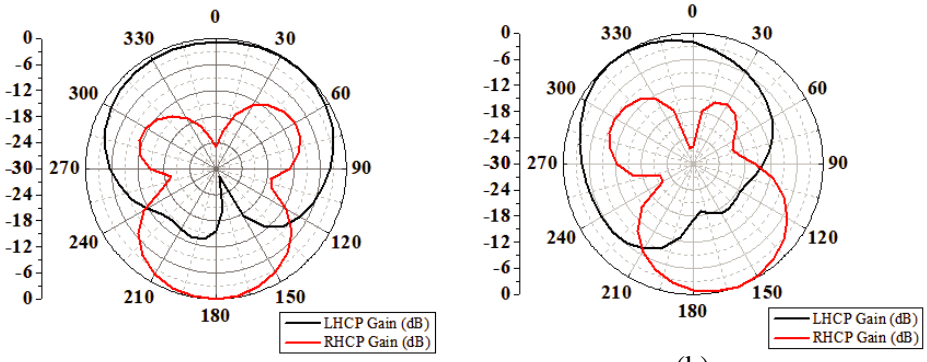

Figure 7. Normalised radiation pattern at 2.45 GHz (a) Phi = 0°. (b) Phi = 90°.

3.4. Specific Absorption Rate

In order to meet basic SAR restrictions for general public exposure (i.e., IEEE C95.1-1999 [1-g averaged SAR < 1.6 W/kg] and IEEE C95.1-2005 [10-g averaged SAR < 2 W/kg]), the power delivered by the antenna has to be modified. The highest SAR value obtained in our analysis is 242 w/Kg for 1 W of input power. Hence, in order to satisfy the most restrictive SAR regulation (i.e., SAR < 1.6 W/kg), the input power must be limited to 6.5 mW. Figure 8 represents the average SAR distribution of the proposed antenna in the single layer tissue model.

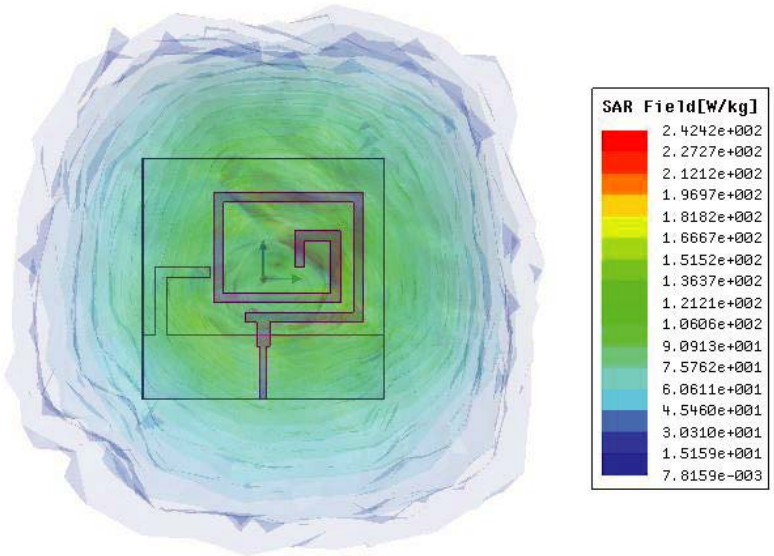

Figure 8. Average SAR analysis for proposed antenna.

3.5. Experimental Verification

The fabricated antenna is depicted in Figure 1(b). To validate the antenna performance, the antenna measurement is performed in a container filled with skin-mimicking gel as shown in Figure 9(a). The dimensions of the skin-mimicking gel during measurement are chosen to be $90 \times 90 \times 25$ mm. Figure 9(b) shows the comparison of the measured and simulated S_{11} of the proposed antenna.

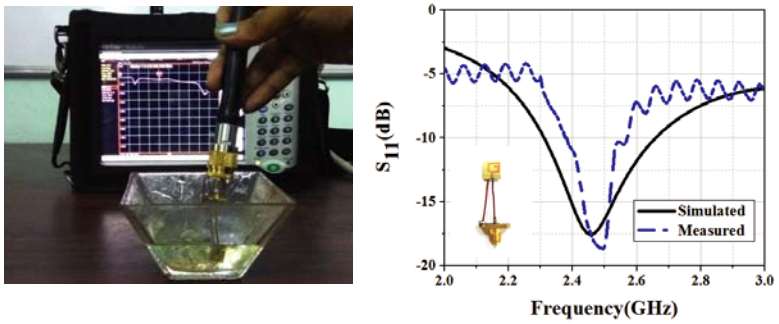

(a) (b)

Figure 9. Measurement setup for the proposed antenna. (a) Implantable monopole antenna inside skin mimicking gel. (b) Simulated and measured reflection coefficient.

As seen in Figure 9(b), both the simulated and measured resonant frequencies are close enough with minimum detuning. The measured antenna bandwidth in skin-mimicking gel is 11% (2.38–2.56 GHz), though covering the desired ISM band, yet relatively narrower than that of the simulated one. This discrepancy is probably due to the fabrication error, solder roughness, the differences in dielectric properties between simulation and measurement, and the cable connected to the antenna during measurement. A brief comparison of the proposed antenna to previous works is shown in Table 2.

Table 2. Comparison of the proposed antenna to prior art.

Ref.	Dimensions (mm×mm×mm)	feed	($S_{11} < -10$ dB), % of impedance Bandwidth	(AR < 3 dB), % of AR Bandwidth	Peak Gain dBi	SAR (W/Kg)
Changrong Liu et al. [11]	10×10×1.27 (127 mm^3)	coax	2.36–2.55 GHz (∼ 7.74%)	2.44–2.48 GHz (∼ 1.63%)	−22	213
Zhi-Jie Yang et al. [13]	10×10×1.27 (127 mm^3)	coax	2.35–2.50 GHz (∼ 6.2%)	2.36–2.56 GHz (∼ 8.13%)	−27	——
Rongqiang Li et al. [14]	11×111×1.27 (153.67 mm^3)	coax	2.31–2.51 GHz (∼ 8.3%)	2.419–2.48 GHz (∼ 2.49%)	−22.7	733.5
Xiong Ying Liu et al. [20]	8.5×8.5×1.27 (91.7575 mm^3)	coax	2.32–2.62 GHz (∼ 12.2%)	2.42–2.48 GHz (∼ 2.4%)	−17.0	210.80
Changrong Liu et al. [21]	$\Pi \times 5.5^2 \times 3.81$ (362.0 mm^3)	coax	2.2–2.8 GHz (∼ 26%)	2.42–2.5 GHz (∼ 33.3%)	−32	180.7
Hua Li et al. [22]	10×10 ×1.27 (127 mm^3)	coax	2.22–2.61 GHz (∼ 16.15%)	2.39–2.54 GHz (∼ 6.09%)	−22.33	254.74
Proposed Work	**10×10×0.3 (30 mm^3)**	**microstrip**	**2.30–2.64 GHz (∼ 13.87%)**	**2.38–2.51 GHz (∼ 5.30%)**	**−7.79**	**242.76**

The volume of the reported antennas in the prior part is larger than our proposed one. In addition, our work exhibits the highest peak gain with better impedance bandwidth than [11, 13, 14, 20] and larger AR bandwidth than others [11, 14, 20]. It is also observed that the SAR (W/Kg) of the proposed antenna is quite good and has an acceptable value.

4. CONCLUSION

Combining the circular polarization designing principle with its miniaturization technique presents an ambitious job for implantable antenna designers. In this paper, the proposed implantable monopole antenna is simple in structure, circularly polarized and covers the intended entire ISM band (2.4–2.48 GHz). Realization of the circular polarization is explained through two antenna prototypes, and their performances are compared extensively. By employing an "L" shaped stub in the ground plane, the proposed antenna evinces circular polarization with reduced volume ($10 \times 10 \times 0.3\,\text{mm}^3$) and peak gain of -7.79 dBi. Finally, the experimental verification is performed, and the measured results are close enough to that of the simulated values. The radiation of the proposed antenna satisfies the health safety regulations and hence, can find its utility in various biomedical applications.

REFERENCES

1. Kiourti, A. and K. S. Nikita, "Implantable antennas: A tutorial on design, fabrication, and in vitro/in vivo testing," *IEEE Microw. Mag.*, Vol. 15, No. 4, 77–91, 2014.
2. Kiourti, A., K. A. Psathas, and K. S. Nikita, "Implantable and ingestible medical devices with wireless telemetry functionalities: A review of current status and challenges," *Wiley Bioelectromagn.*, Vol. 35, No. 1, 1–15, 2014.
3. Lee, M. C., T.-C. Yo, F.-J. Huang, and C.-H. Luo, "Dual-resonant P-shape with double L-strips PIFA for implantable biotelemetry," *Electronics Letters*, Vol. 44, No. 14, 2008.
4. Kim, J. and Y. Rahmat-Samii, "Planar inverted-F antennas on implantable medical devices: Meandered type versus spiral type," *Microwave and Optical Technology Letters*, Vol. 48, No. 3, 2006.
5. Basari, D. C. S., F. Y. Zulkifli, and E. T. Rahardjo, "A helical folded dipole antenna for medical implant communication applications," *IEEE MTT-S International Microwave Workshop Series on RF and Wireless Technologies for Biomedical and Healthcare Applications (IMWS-BIO)*, 2013.
6. Rula, S. A., Y. Huang, M. Kod, and A. A. BakarSajak, " A broadband flexible implantable loop antenna with complementary split ring resonators," *IEEE Antennas and Wireless Propagation Letters*, Vol. 14, 1506–1509, 2015.
7. Liu, C., Y.-X. Guo, and S. Xiao, "A hybrid patch/slot implantable antenna for biotelemetry devices," *IEEE Antennas and Wireless Propagation Letters*, Vol. 11, 2012.
8. Permana, H., Q. Fang, and W. S. T. Rowe, "Hermetic implantable antenna inside vitre-ous humor simulating fluid," *Progress In Electromagnetics Research*, Vol. 133, 571–590, 2013.
9. Garcia-Miquel, A., S. Curto, N. Vidal, J. M. Lopez-Villegas, F. M. Ramos, and P. Prakash, "Multilayered broadband antenna for compact embedded implantable medical devices: Design and characterization," *Progress In Electromagnetics Research*, Vol. 159, 1–13, 2017.
10. Gao, S. (S.), Q. Luo, and F. Zhu, *Circularly Polarized Antennas*, John Wiley & Sons Ltd, University of Kent, UK, 2014.
11. Liu, C., Y.-X. Guo, and S. Xiao, "Capacitively loaded circularly polarized implantable patch antenna for ISM band biomedical applications," *IEEE Ttransactions on Antennas and Propagation*, Vol. 62, No. 5, 2014.
12. Xu, L.-J., Y.-X. Guo, and W. Wu, "Miniaturized circularly polarized loop antenna for biomedical applications," *IEEE Transactions on Antennas and Propagation*, Vol. 63, No. 3, 2015.
13. Yang, Z.-J., S.-Q. Xiao, L. Zhu, B.-Z. Wang, and H.-L. Tu, "A circularly polarized implantable antenna for 2.4 GHz ISM band biomedical applications" *IEEE Antennas and Wireless Propagation Letters*, Vol. 16, 2554–2557, 2017.
14. Li, R., Y.-X. Guo, B. Zhang, and G. Du, "A miniaturized circularly polarized implantable annular-ring antenna," *IEEE Antennas and Wireless Propagation Letters*, Vol. 16, 2566–2569, 2017.
15. Duan, Z. and L.-J. Xu, "Dual-band implantable antenna with circular polarisation property for ingestible capsule application," *Electronics Letters*, Vol. 53, No. 16, 1090–1092, 2017.

16. Ding, K., C. Gao, T. Yu, and D. Qu, "Broadband C-shaped circularly polarized monopole antenna," *IEEE Transactions on Antennas and Propagation*, Vol. 63, No. 2, 2015.
17. Ding, K., Y.-X. Guo, and C. Gao, "CPW-fed wideband circularly polarized printed monopole antenna with open loop and asymmetric ground plane," *IEEE Antennas and Wireless Propagation Letters*, Vol. 16, 2017.
18. Saini, R. K., S. Dwari, and M. K. Mandal, "CPW-fed dual-band dual-sense circularly polarized monopole antenna," *IEEE Antennas and Wireless Propagation Letters*, Vol. 16, 2017.
19. Agbinya, J. I., *Wireless Power Transfer*, Edition: 1, Chapter 10, "Wireless Powering and Propagation of Radio Frequencies through Tissue", 301–336, 2012.
20. Liu, X. Y., Z. T. Wu, Y. Fan, and E. M. Tentzeris, "A miniaturized CSRR loaded wide-beamwidth circularly polarized implantable antenna for subcutaneous real-time glucose monitoring," *IEEE Antennas and Wireless Propagation Letters*, Vol. 16, 2017.
21. Liu, C., Y.-X. Guo, and S. Xiao "Circularly polarized helical antenna for ism-band ingestible capsule endoscope systems," *IEEE Transactions on Antennas and Propagation*, Vol. 62, 2014.
22. Li, H., Y.-X. Guo, and S.-Q. Xiao, "Broadband circularly polarised implantable antenna for biomedical applications," *Electronics Letters*, Vol. 52, No. 7, 504–506, 2016.